


 Cite this: *RSC Adv.*, 2024, 14, 24845

# Design of a double-layered material as a long-acting moisturizing hydrogel–elastomer and its application in the field protection of elephant ivories excavated from the Sanxingdui Ruins

 Lang Jiang,<sup>a</sup> Shilin Xiang,<sup>a</sup> Xiaoying Ji,<sup>b</sup> Jinshan Lei,<sup>b</sup> Dongliang Li,<sup>b</sup> Sifan Li,<sup>c</sup> Lin Xiao,<sup>d</sup> Luman Jiang,<sup>d</sup> Lijuan Zhao<sup>\*a</sup> and Yi Wang <sup>\*a</sup>

The sudden change in the environment from a dark, low-oxygen, low-temperature, high-humidity underground stable environment to an environment with much-improved temperature and humidity, a high oxygen content, enhanced light exposure, and increased harmful organisms has greatly affected the stability of the ivory unearthed from the Sanxingdui site. Therefore, the implementation of an effective emergency protection strategy for ivory excavated at Sanxingdui is imperative and urgently needed. However, the current gauze technique used at many archaeological sites suffers from short timescales, poor transparency of the material, and susceptibility to reverse osmosis of the ivory. Therefore, in this study, a transparent poly(acrylamide-acrylic acid) (P(AM-AA)) hydrogel-poly(dimethylsiloxane) (PDMS) elastomer bilayer was designed for the effective protection of excavated ivory. In this system, a hydrophobic PDMS elastomer was constructed on the surface of the hydrogel by the introduction of a silane coupling agent to inhibit the loss of water from the hydrogel to the external environment, thus prolonging the preservation of ivory by the protective material. The covalent interface between the hydrogel and the elastomer allowed the double-layer composite to exhibit excellent interfacial bonding. In addition, the double-layer material demonstrated a high mechanical strength of 1.2 MPa and a water binding ratio of ~31%, which allowed it to form strong hydrogen bonds with the silanol structure. When the hydrogel was placed in an air environment (temperature: 25 °C; relative humidity: 65% RH), the water-retention rate of the double-layer material was still more than 60% after 5 days, thus the double-layer material showed excellent performance. Meanwhile, the double-layer material had a transmittance of more than 90% and exhibited a high degree of transparency, which makes it possible to promptly observe the changes occurring on the surface of the ivory. The combination of the aforementioned properties makes the bilayer a promising material for moisturizing and protecting excavated ivory *in situ*. Based on these properties, we used the prepared P(AM-AA)/PDMS double-layer material directly for wrapping the K8 ivory with the highest water content at Sanxingdui. The weight retention rate of the ivory was around 70% after 50 days of placement (temperature: 25 °C; relative humidity: 60% RH), the macroscopic morphology did not change significantly and the mechanical properties of the wrapped ivory were basically unchanged, which indicated that the double-layer material has an excellent on-site protection effect on the ivory excavated from Sanxingdui. This work provides new ideas and methods for the temporary conservation of wet heritage.

 Received 28th May 2024  
 Accepted 18th July 2024

DOI: 10.1039/d4ra03919j

[rsc.li/rsc-advances](http://rsc.li/rsc-advances)

## Introduction

Excavated dental and bony artifacts, such as the bones and teeth of ancient humans and animals, as well as various bone tools, are witnesses of history. They carry the imprint of human civilization and the traces of natural evolution. Excavated ivory is one such typical dental and bony artifact. So far, a total of 8 sacrificial pits have been found in the Sanxingdui Ruins.<sup>1</sup> Elephant tusks and ivory artifacts unearthed from the Sanxingdui site in Guanghan and the Jinsha site in Chengdu,

<sup>a</sup>College of Chemistry and Materials Science, Sichuan Normal University, Chengdu 610068, China. E-mail: [lijuan\\_zhao@sicnu.edu.cn](mailto:lijuan_zhao@sicnu.edu.cn); [wangyi2020@sicnu.edu.cn](mailto:wangyi2020@sicnu.edu.cn)
<sup>b</sup>Cigar Fermentation Technology Key Laboratory of China Tobacco, Industrial Efficient Utilization of Domestic Cigar Tobacco Key Laboratory of Sichuan Province, China Tobacco Sichuan Industrial Co., Ltd, Chengdu 610066, China

<sup>c</sup>Sichuan Province Institute of Cultural Relics and Archeology, Chengdu 610041, China

<sup>d</sup>Chengdu Institute of Cultural Relics and Archaeology, Chengdu 610072, China


China, are approximately 3000 years old. The quantity and cultural value of these artifacts are extremely rare on a global scale.<sup>2</sup> The ivories unearthed from the Sanxingdui Relics site were basically in a water-saturated state and contained a large amount of water. These newly unearthed ivories can be greatly affected by changes in the environment, including temperature, humidity, an increase in light intensity, and an increase in oxygen content, which can have a great impact on the stability of the ivories. Without reasonable and effective emergency protection measures, the moisture inside the ivories will rapidly evaporate until they are completely dehydrated, causing discoloration, deformation, cracking, and ultimately pulverization of the ivories. Additionally, after being unearthed, many microorganisms, such as mold and bacteria, proliferate inside the ivories. These harmful microorganisms further erode the main inorganic components of the ivories, causing irreversible damage.<sup>3</sup> Therefore, it is a significant task with great practical significance to effectively protect the unearthed ivories.

As for the emergency protection of unearthed ivories, there are few related reports abroad. Domestically, Chengdu Institute of Archaeology was the first to use gauze moisture-retention technology to lock and maintain the moisture of unearthed ivories from the Jinsha Ruins, or use silicone material sealing technology to preserve unearthed ivories. The Chengdu Institute of Archaeology previously used silicone materials to temporarily protect ancient ivories unearthed from the Jinsha Ruins. In this process, during the initial stage of sealing and protection with silicone materials, the moisture of the ivories was almost completely locked in, allowing them to be preserved in an environment close to their original burial conditions for a period of time. This not only significantly reduced the rate of water loss from the ancient ivories but also isolated them from harmful gases and microorganisms that were present in the outside environment. The initial results of this sealing and the protection method were remarkable.<sup>4–6</sup> The current preservation technique involves wrapping the ivory in two layers of plastic wrap, wetting the polymer bandage with ion-exchange water, and then uniformly applying this to the surface of the ivory. After the polymer bandage solidifies, a saturated and sterilized wet cotton pad is applied to maintain the humidity of the ivory.<sup>7</sup> However, due to the poor water resistance of the polymer bandage, the current method can cause reverse osmosis due to the imbalance of the water content between the ivory and the wrapping material after a long period of time. In addition, the plaster used to fix the ivory will absorb a certain amount of water. Therefore, the preservation time of the ivory is not long and its ornamental value may be greatly reduced, which is not conducive to its exhibition and observation. Therefore, to carry out effective research and development into emergency protection materials, there is an urgent need to formulate corresponding emergency moisturizing materials for different excavated ivories, to solve the problem of the temporary protection and on-site preservation of excavated ivories during archaeological excavations, and to lay a foundation for their subsequent preservation and research.

As wet and soft polymer materials with a three-dimensional polymer network containing a large amount of water, hydrogels

have the advantages of an adjustable network structure and water content, as well as allowing an easy control of their mechanical properties.<sup>8–17</sup> Their wide range of applications and properties suggests they would be effective emergency protective materials for excavated ivories. However, hydrogels gradually lose water when exposed to air or dry environments, leading to a loss of their flexibility, elasticity, and corresponding functions. Therefore, inhibiting water evaporation, enhancing the water-retention capacity of hydrogels, and improving their stability are crucial for prolonging their usage duration.<sup>18,19</sup> Moreover, to further extend the effective moisturizing duration of emergency protective materials for excavated ivories, such as those from the Sanxingdui site, a hydrophobic elastomer layer, inspired by the structure of skin, was investigated and modified on the surface of the hydrogel to block water loss from the hydrogel.<sup>20–22</sup> This allowed the hydrogel to form a dynamic moisture regulation mechanism with the water-saturated ivory under relatively stable humidity conditions. However, bonding hydrophobic materials like elastomers with hydrophilic materials like hydrogels is a significant challenge.<sup>23,24</sup> Zhu *et al.*<sup>20</sup> proposed an effective method of interfacial bonding for addressing the weak interfacial mechanical properties between hydrogels and elastomers, which raised the interfacial energy to more than  $1000 \text{ J m}^{-2}$  and demonstrated potential application in functional microstructures. Wirthl *et al.*<sup>25</sup> developed a rapid and effective interface bonding method that could be used for the adhesion of hydrogels with hydrogels, plastics, elastomers, leather, bone, and metal. Silane coupling agents are commonly used coupling materials for connecting inorganic materials with organic materials.<sup>26,27</sup> Silane coupling agents can undergo hydrolysis, where the alkoxy groups hydrolyze to form silanols, which can chemically bond with inorganic substances. On the other hand, the organic functional groups can react with reactive groups in organic materials.<sup>28</sup> Therefore, this study designed a transparent double-layered material of P(AM-AA)/PDMS elastomer, which involved constructing a hydrophobic polydimethylsiloxane (PDMS) elastomer layer on the surface of the hydrogel to inhibit the loss of water from the hydrogel to the environment, thereby prolonging the preservation time of elephant ivory while serving as an emergency moisturizing material. The introduced coupling agent exhibited excellent interfacial bonding at the covalent interface between the hydrogel and the elastomer, and the prepared double-layered moisturizing material demonstrated an excellent on-site moisturizing ability during the temporary preservation of elephant ivory.

## Experimental section

### Materials

Acrylamide (AM) and glycerol (Gly) were provided by Chengdu Huaxia Chemical Reagent Ltd, China. Acrylic acid (AA) and 2-hydroxy-2-methyl-1-phenyl-1-propanone (HMPP) were acquired from Tokyo Chemical Industry Co., Ltd, Japan. 3-(Trimethoxysilyl)propyl methacrylate (TMSPMA) and sodium dodecyl sulfate (SDS) were provided by Chengdu Kelong Chemical Co., Ltd, China. Divinyl-terminated polydimethylsiloxane (PDMS,



Sylgard 184) and 2,4,6,8-tetramethylcyclotetrasiloxane (D4H) were acquired from Dow Corning Corporation. All the reagents in this study were used as received. Deionized (DI) water was used throughout this work.

#### Preparation of the P(AM-AA)/PDMS double-layered material.

The PDMS precursor solution was obtained by mixing PDMS raw materials and D4H curing agent in a certain mass ratio. Then, 200  $\mu\text{L}$  of TMSPMA was added to the PDMS precursor solution using a pipette, and magnetically stirred for 20 min to mix uniformly. After that, the solution was poured into a polypropylene mold for leveling, and left to stand at room temperature for 10 min. After the bubbles had stopped completely, the mold was placed in a 100  $^{\circ}\text{C}$  oven for thermal curing for 30 min to obtain the PDMS elastomer. Certain amounts of AM and AA monomers were dissolved in a binary solvent of deionized water and glycerol (Gly). Also, a certain amount of TMSPMA was used as a coupling agent, which was measured using a pipette. By controlling the amount of AA, the pH value of the precursor solution was maintained at pH 4–5, facilitating the better dissolution and hydrolysis of TMSPMA. The spontaneous condensation of TMSPMA hydrolysis led to the formation of silanol structures, which served as cross-linking points within the gel, thus acting as a cross-linking agent. To further promote the dissolution and hydrolysis of the coupling agent, sodium dodecyl sulfate (SDS) was added to the mixed solution. The mixture was then thoroughly stirred to form a uniform and transparent solution. The prepared mixed solution was cast onto the already cured PDMS surface, followed by polymerization of the P(AM-AA) hydrogel under UV light. Finally, the entire assembly was placed in a 30  $^{\circ}\text{C}$  oven for 1 day. To ensure that the hydrogel could maintain its structural integrity and moisturizing effect during its subsequent application for the temporary protection of ivory excavated from the Sanxingdui site, we specifically designed the water content of the hydrogel to be similar to that of the ivory; thereby ensuring that water could be transmitted in an optimal state and minimizing any potential negative impacts. By adjusting the concentration of the curing agent in PDMS, three different cross-linking densities of PDMS were prepared. These PDMS samples were then bonded with P(AM-AA) hydrogels to create a bilayer structure material composed of the hydrogel and elastomer. The samples were named P(AM-AA)/PDMS- $x$ , where “ $x$ ” represents the ratio of the raw material to the curing agent in PDMS.

**Composition analysis of the double-layered material.** The infrared spectrum of the P(AM-AA)/PDMS double-layer material was recorded using a Thermo Scientific Nicolet iS50 FTIR instrument operated in the attenuated total reflection (ATR) mode. The instrument resolution was 4  $\text{cm}^{-1}$ , the number of scans was 32, and the test wave number range was from 4000  $\text{cm}^{-1}$  to 400  $\text{cm}^{-1}$ .

**Adhesion performance of the double-layered material.** The cross-sectional structure of the hydrogel/elastomer double-layered material after freeze-drying was observed by scanning electron microscopy (SEM, Zeiss EV018, Carl Zeiss Optics, China), and the cross-section of the double-layered material was observed by optical microscopy (POLYVAR-MET, Changsha Aikexipu Instrument and Equipment Co. Ltd, China). The

double-layered material was stretched to twice its original length using a universal testing machine (Instron 3367, Instron (Shanghai) Testing Equipment Trading Co. Ltd, China), and it was observed whether the hydrogel and the elastomer separated.

**Optical properties of the double-layered material.** The hydrogel, elastomer, and hydrogel/elastomer double-layered material were all cut into rectangular shapes with a thickness of 2 mm. Then the samples were scanned and tested using an ultraviolet-visible absorption spectrometer (UV-Vis, Ulspec 7000, PerkinElmer, UK). The wavelength range of the test was 400–800 nm.

**Mechanical properties of the double-layered material.** The mechanical properties of the P(AM-AA) hydrogel and P(AM-AA)/PDMS double-layered material were characterized using a tensile testing machine at room temperature. The operation method was as follows: first, the dumbbell-shaped specimen was clamped on the tensile machine. The initial gauge length of the specimen was 20 mm, the width was 2 mm, and the thickness was 2 mm. The specimen was stretched at a constant tensile rate of 100  $\text{mm min}^{-1}$ , and the corresponding tensile stress–strain curve was recorded. For the rheological tests (MCR 302, Anton Paar Co. Ltd, China) of the elastomer materials, the PDMS elastomer was cut into circular specimens with a diameter of 25 mm. Strain sweep tests were conducted at a constant frequency of 10  $\text{rad s}^{-1}$  within a strain range of 0.1–100%. Frequency sweep tests were also performed at a fixed strain of 0.1% within a frequency range of 0.1–100  $\text{rad s}^{-1}$ .

**Moisture-retention properties of the double-layered material.** The water-retention properties of the P(AM-AA)/PDMS double-layered material and single-layer P(AM-AA) hydrogels were tested by a weighing method. The samples were placed under conditions of 25  $^{\circ}\text{C}$  temperature and 60% relative humidity, and their weights were recorded every day using an electronic balance (ME203, Mettler-Toledo Instruments Co. Ltd, China). Immediately after weighing, the samples were returned to their original positions. The water-retention rates of the samples were determined using the following formula:

$$\text{WR} = \frac{W_t}{W_0} \times 100\% \quad (1)$$

where WR refers to the water-retention rate,  $W_0$  refers to the initial weight of the sample, and  $W_t$  refers to the weight of the sample after  $t$  day. To ensure the validity of the test results, each group of samples was tested three times and the average value was taken.

A dynamic water vapor sorption analyzer (Puyoumidi SPS11-10 $\mu$ , Proumid GmbH, Germany) was used to measure the dehydration kinetics of the double-layered materials, in which the gradient was set to 15% RH/45 min, and the test temperature was set to a constant temperature of 25  $^{\circ}\text{C}$ .

Using a low-field nuclear magnetic resonance analyzer (LF-NMR, MesoMR23-060H-I, Newmark Analytical Instruments Co. Ltd, Suzhou, China), the water state and its proportion of the double-layered hydrogel material were tested. The resonance frequency was set to 23 MHz, and the magnetic field strength was 0.5 T. At the same time, in order to fully consider



the potential impact of temperature on the moisture content of the hydrogel materials,<sup>29</sup> and the environmental conditions in the practical application of subsequent double-layered materials in the temporary protection of unearthed ivory, we strictly controlled the test temperature at room temperature. Finally, the obtained test data was inverted 10 000 times and the transverse relaxation time  $T_2$  map was successfully obtained.

**Field study on the protection of excavated ivory with the double-layered material.** Using an ultradepth three-dimensional microscopy system (VHX-2000C, Keyence Corporation, Japan), the surface morphology of the excavated ivory before and after water loss was observed at different magnifications without protection, using the existing gauze wrapping technology, and using the double-layered hydrogel material protection.

The water-retention performance of the P(AM-AA)/PDMS double-layered material used with the excavated ivory was characterized by weight measurement. The ivory wrapped with the double-layered hydrogel material was placed under the conditions of 25 °C temperature and 60% relative humidity. The weight was recorded every day using an electronic balance, and the sample was immediately returned to its original position after weighing. The water-retention rate of the sample can be expressed by the following formula:

$$WR = \frac{W_n}{W_0} \times 100\% \quad (2)$$

where WR represents the water-retention rate,  $W_0$  represents the initial weight of the ivory, and  $W_n$  represents the weight of the ivory after  $n$  days. To ensure the validity of the test results, each group of samples was tested three times and the average value was taken.

The water-loss-degradation performance of ivory protected by the P(AM-AA)/PDMS double-layered material was tested using a nanoindentation tester (Anton Paar UNHT, Austria). The loading and unloading rates were both 6 mN min<sup>-1</sup>, and the maximum loading force was set to 1 mN. Parallel tests were conducted on three points of each of the four water-saturated

ivories, and the Oliver–Pharr method was used for the quantitative hardness and elastic modulus calculations.

## Results and discussion

Inspired by the structure of skin,<sup>30</sup> a layer of PDMS hydrophobic elastomer was constructed on the surface of the hydrogel to prepare a P(AM-AA)/PDMS double-layered material, which was then used to prolong the preservation period of ivory by the action of the hydrogel, whereby it was applied for the on-site protection of unearthed ivory from the Sanxingdui Ruins site (Fig. 1). A silane coupling agent (TMSPMA) was added to the precursor solutions of the hydrogel and elastomer, respectively, and introduced into the networks of the hydrogel and elastomer through copolymerization. Then, SDS was added to promote the bonding of the silane coupling agent at the interface between the hydrogel and elastomer.<sup>31,32</sup>

TMSPMA plays a pivotal role in the formation of a robust interface between the P(AM-AA) hydrogel and the PDMS elastomer. TMSPMA possesses a unique molecular structure, comprising a methacrylate group (capable of copolymerization with the hydrogel and elastomer precursors) and trimethoxysilyl groups that hydrolyze to form reactive silanol groups. Upon addition to the precursor solutions of both the hydrogel and elastomer, TMSPMA undergoes two key reactions.<sup>33</sup> First, the methacrylate group participates in the copolymerization reactions within the hydrogel and elastomer matrices, integrating the silane molecules into both networks. This copolymerization ensures that TMSPMA is firmly anchored within the polymer matrices, preventing phase separation and enhancing the mechanical integrity of the composite material. Second, the trimethoxysilyl groups of TMSPMA are hydrolyzed in the presence of moisture to form silanol groups. These silanol groups can undergo condensation reactions with each other across the hydrogel–elastomer interface, leading to the formation of siloxane bonds. The introduction of SDS facilitates this process by improving the miscibility of the silane coupling agent at the interface, enhancing the efficiency of the silanol condensation

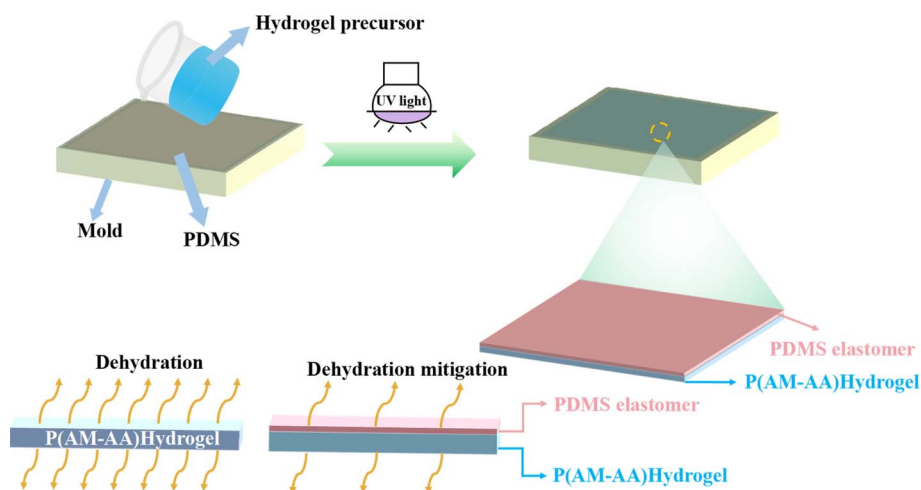


Fig. 1 Schematic diagram for the preparation of the P(AM-AA)/PDMS double-layered material.



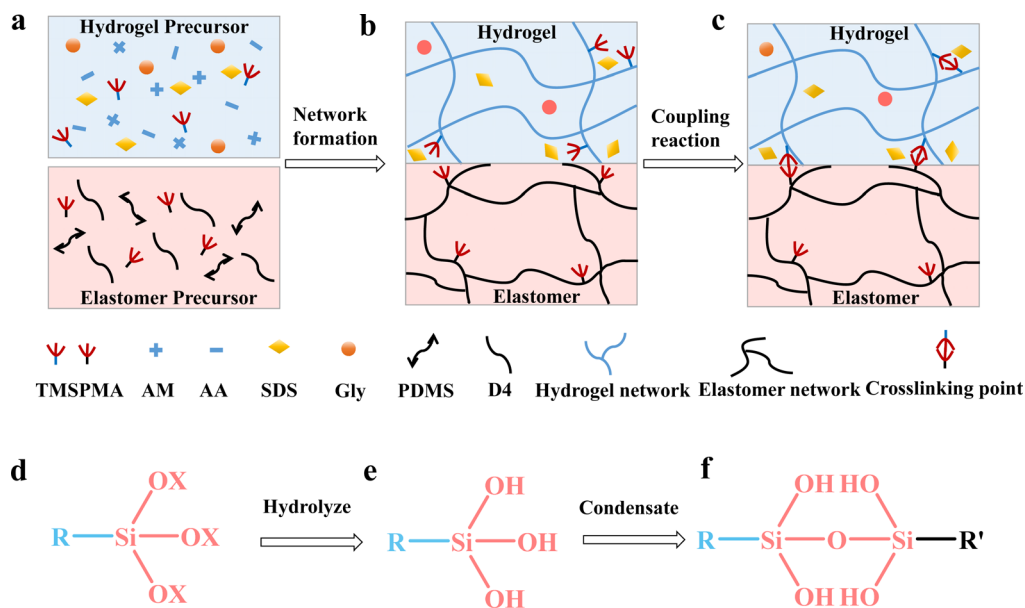


Fig. 2 Schematic diagram of the principle of the *in situ* bonding method for soft materials. (a) TMSi(OR)<sub>3</sub> is mixed separately into precursor solutions of the hydrogel and elastomer; (b) during the formation of the polymer network, TMSi(OR)<sub>3</sub> is incorporated into the network but remains uncondensed; (c) condensation reactions occur between the TMSi(OR)<sub>3</sub> molecules, forming cross-linking points within the network and generating adhesion at the interface; (d) hydrolysis of the TMSi(OR)<sub>3</sub> leads to the production of (e) silanol; (f) condensation of silanol with silanol generates siloxane.

reactions. The resultant siloxane bonds formed across the interface provide a strong, covalent linkage between the hydrogel and elastomer layers.<sup>34</sup> The mechanism is shown in Fig. 2 (where  $R/R'$  in Fig. 2d–f represents the organic groups in TMSi(OR)<sub>3</sub>, and  $X$  represents the methyl group in TMSi(OR)<sub>3</sub>). This covalent bonding is critical for the durability and mechanical stability of the P(AM-AA)/PDMS double-layered material. It ensures that the composite material can withstand the stresses and strains encountered during the preservation and on-site protection of archaeological finds, such as the ivory from the Sanxingdui Ruins site.

In summary, the integration of TMSi(OR)<sub>3</sub> into the hydrogel and elastomer networks through copolymerization, followed by the formation of covalent siloxane bonds *via* silanol condensation at the interface, is central to achieving a durable and robust bond between the hydrogel and PDMS layers. This molecular mechanism underpins the effectiveness of the P(AM-AA)/PDMS double-layered material in prolonging the preservation of ivory artifacts by providing both hydrophobic protection and mechanical support.

In this study, a layer of PDMS hydrophobic elastomer was constructed on the surface of a hydrogel to prolong the preservation period of hydrogel elephant ivory and was applied for the on-site protection of elephant ivory unearthed from the Sanxingdui Ruins site. Fig. 3c shows the infrared absorption spectra of P(AM-AA)/PDMS double-layer material (on the side of hydrogel), P(AM-AA) hydrogel, and PDMS elastomer. Peaks could be observed at 2954 and 2850  $\text{cm}^{-1}$  ( $-\text{CH}_2$  stretching vibration),<sup>35,36</sup> 1663  $\text{cm}^{-1}$  ( $\text{C}=\text{O}$  stretching vibration), 1605  $\text{cm}^{-1}$  ( $\text{N}-\text{H}$  bending vibration), and 1103  $\text{cm}^{-1}$  ( $\text{C}-\text{OH}$  stretching vibration peak) in the infrared spectrum of the P(AM-

AA)/PDMS double-layered material.<sup>37</sup> In addition, the characteristic peak at 1260  $\text{cm}^{-1}$  in the infrared spectrum of PDMS was attributed to the bending vibration absorption peak of  $\text{Si}-\text{CH}_3$ , reflecting the connection between silicon atoms and methyl groups in the molecule. The strong peak at 2963  $\text{cm}^{-1}$  was attributed to the asymmetric stretching vibration of  $-\text{CH}_3$  in PDMS, while the absorption peak at 785  $\text{cm}^{-1}$  was related to the stretching vibration of  $\text{Si}-\text{O}$  in the PDMS molecular chain.<sup>38</sup> In the infrared spectrum of the P(AM-AA)/PDMS double-layered material, the peak at 2963  $\text{cm}^{-1}$  was shifted to a lower wavelength, while the characteristic peak at 785  $\text{cm}^{-1}$  exhibited a red-shift, which was due to the hydrolysis of the silane coupling agent in PDMS.<sup>39,40</sup>

When manually peeling the hydrogel off the surface of PDMS elastomer, it was not difficult to find significant hydrogel residue on the elastomer (Fig. 3a). At the same time, when the overall double-layered material was stretched to twice its original length by a tensile tester, no separation between the hydrogel and the elastomer was observed (Fig. 3b). In addition, by observing the cross-sectional structure of the P(AM-AA)/PDMS double-layered material through SEM and optical microscopy, it could be seen that the hydrogel and the elastomer were tightly combined, exhibiting a distinct double-layered structure (Fig. 3d and e). The above results indicate that there was good interfacial bonding between the P(AM-AA) hydrogel and the PDMS elastomer, enabling the successful modification of the hydrophobic elastomer layer on the surface of the hydrogel.

The protective material for unearthed ivory should ensure its transparency, meaning it should have good light transmittance, to facilitate the display of ivory cultural relics and observation of



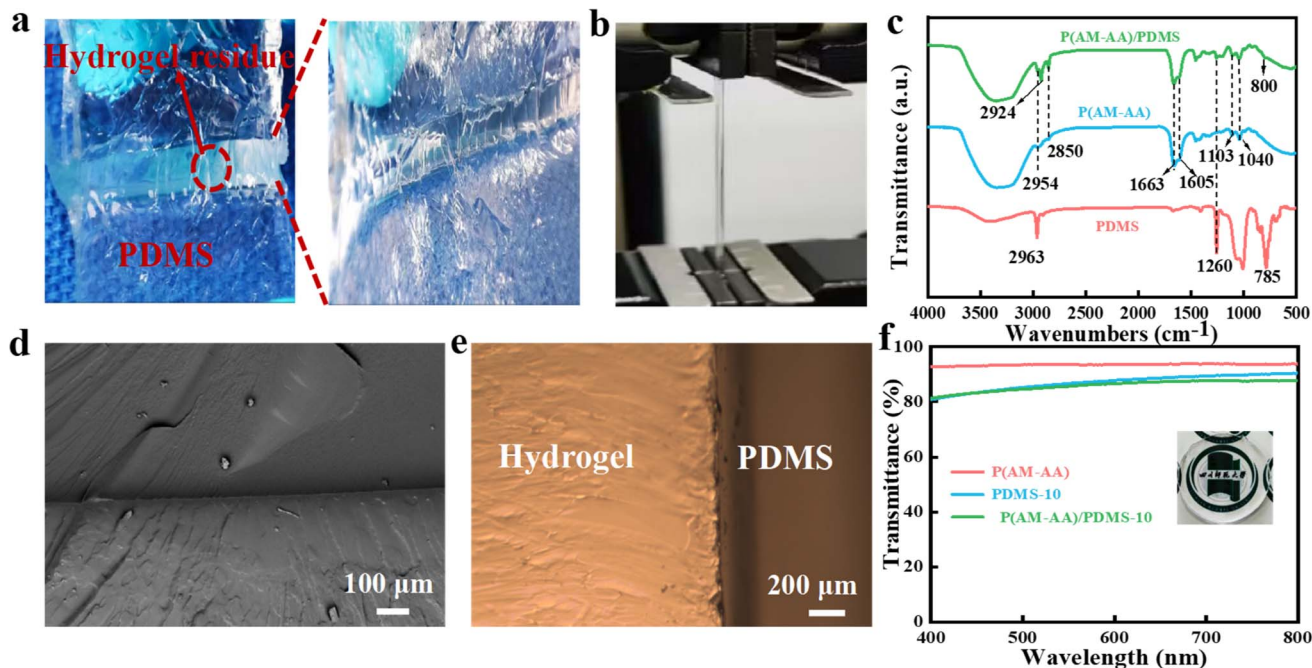


Fig. 3 (a) Photograph of peeling the hydrogel from the surface of the PDMS elastomer; (b) photograph of stretching the double-layered material to twice the original length; (c) FTIR spectra of P(AM-AA)/PDMS, P(AM-AA), and PDMS; (d) SEM image and (e) optical microscope image of P(AM-AA)/PDMS; (f) UV-vis transmittance spectra of P(AM-AA)/PDMS, P(AM-AA), and PDMS.

their condition during storage. As shown in Fig. 3f, the transmittance spectra of the P(AM-AA) hydrogel, PDMS elastomer, and P(AM-AA)/PDMS double-layered material were tested using a UV absorption spectrometer. The transmittance of the hydrogel at 600 nm was 93.5%, and that of the elastomer was 87.8%, both of which showed excellent transmittance. The transmittance of the composite after bonding the hydrogel and elastomer was 86.6% at 600 nm, and could reach 94% at 800 nm, indicating the transparency was still very high. When placing the P(AM-AA)/PDMS double-layered material on a paper with the words “Sichuan Normal University” printed on it, the words on the paper could be clearly seen (Fig. 3f). Compared with the traditional gauze moisturizing method, the transparent moisturizing material is convenient for directly observing the physical state of the excavated ivory surface and the growth state of mold, while the excellent transparency also indicates that the polymers within the hydrogel do not undergo phase separation under room temperature conditions, which is conducive to the efficient protection of the excavated ivory.

By varying the ratio of the PDMS raw material to the curing agent, three PDMS elastomers with different cross-linking densities were prepared. Initially, the structural differences in the PDMS networks were characterized through tensile testing. It could be observed that PDMS-5, due to its highest proportion of curing agent, exhibited a higher cross-linking density and a denser network structure,<sup>41</sup> resulting in excellent mechanical properties with a tensile strength of 6.5 MPa, elastic modulus of 1.5 MPa, and toughness of 4.2 MJ m<sup>-3</sup>. As the concentration of the curing agent decreased, the cross-linked network became more loosely packed, leading to an increase in fracture strain

and decreases in the tensile strength, modulus, and toughness (Fig. 4a–c). By constructing a layer of PDMS hydrophobic elastomer on the surface of the hydrogel, three double-layered materials with different cross-linking densities of PDMS elastomer and P(AM-AA) hydrogel were prepared, namely P(AM-AA)/PDMS-5, P(AM-AA)/PDMS-10, and P(AM-AA)/PDMS-15. By comparing the mechanical properties of the pure P(AM-AA) hydrogel with the P(AM-AA)/PDMS double-layered materials, we found that the tensile strength of the pure P(AM-AA) hydrogel was approximately 38 kPa. However, after modifying with a layer of PDMS elastomer, the mechanical properties of the overall double-layered material were significantly improved. In particular, P(AM-AA)/PDMS-5, due to its highest proportion of curing agent, had a larger cross-linking density and a tighter network structure, resulting in a tensile strength of 1.2 MPa, elastic modulus of 3.1 MPa and toughness of 0.8 MJ m<sup>-3</sup>. As the concentration of the curing agent decreased, the cross-linked network became looser, leading to a decrease in both tensile strength and modulus. However, the fracture strain and toughness (1.2 MJ m<sup>-3</sup>) of P(AM-AA)/PDMS-10 both increased (Fig. 4d–f). These results indicate that P(AM-AA)/PDMS double-layered materials possess excellent mechanical properties, suggesting they would be suitable for use in the protection of unearthed wet ivory. However, the long-term exposure of ivory to low temperatures and damp environments results in its fragility and susceptibility to cracking and powdering after excavation. Additionally, the curved shape and fragile nature of the ivory itself can pose further challenges. Therefore, in our next steps, we plan to select the P(AM-AA)/PDMS-10 double-layered material, which has a moderate elastic modulus and



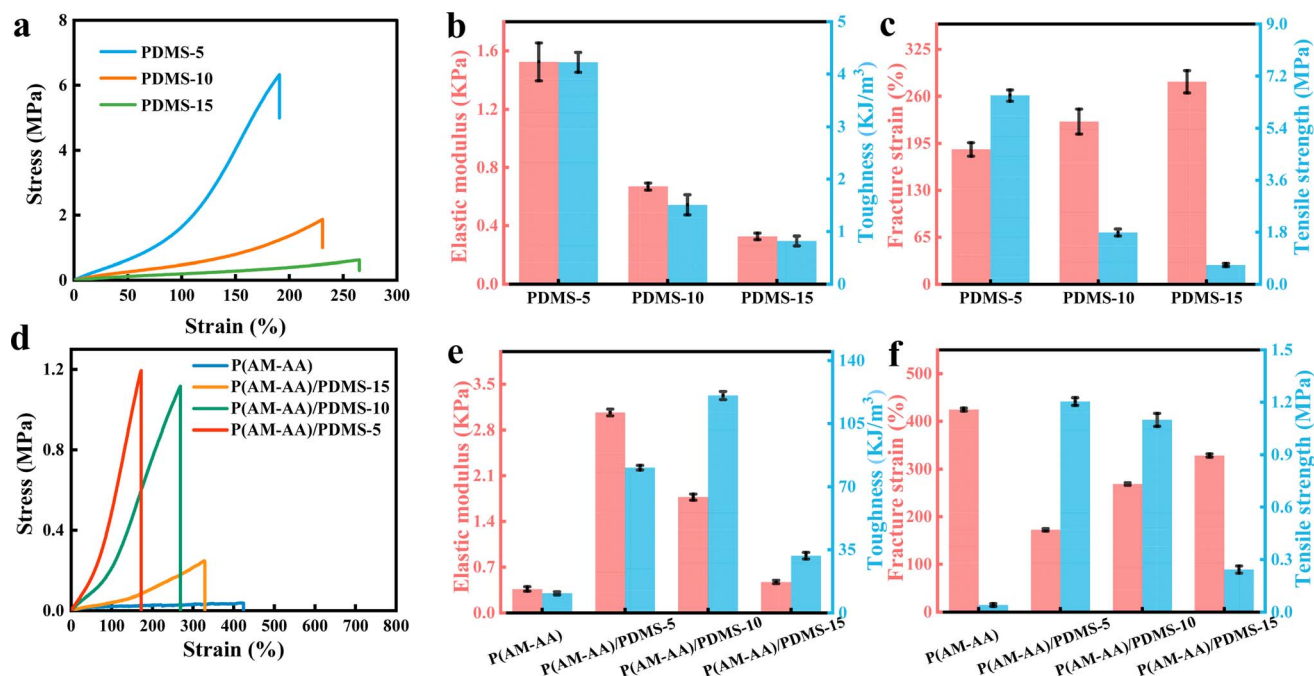


Fig. 4 Mechanical properties of the PDMS samples. (a) Tensile stress–strain curves of the PDMS elastomers, (b) comparison of their elastic modulus and toughness, (c) comparison of their fracture strain and tensile strength. Mechanical properties of the P(AM-AA) hydrogel and P(AM-AA)/PDMS bilayer materials. (d) Tensile stress–strain curves of the P(AM-AA) hydrogels and P(AM-AA)/PDMS double-layered material, (e) comparison of their elastic modulus and toughness, (f) comparison of their fracture strain and tensile strength.

strong toughness, as the protective material for the unearthed ivory from the Sanxingdui site for further research.

In this study, the water-retention capacities of the P(AM-AA)/PDMS double-layered materials and monolayer P(AM-AA) hydrogel were tested using the gravimetric method. The monolayer P(AM-AA) hydrogel lost water after being placed in the environment for 1 day, whereby the weight retention rate decreased to ~54%, and then at 5 days, the weight retention rate had decreased to ~45%. However, after a layer of elastomer was constructed on the surface of the hydrogel, the P(AM-AA)/PDMS double-layered material maintained more than 80% of its weight after 1 day, and still maintained ~60% after 5 days. The moisture retention of the hydrogel material after elastomer modification was thus significantly improved (Fig. 5a). Comparing different cross-linking densities, it could be found that as the PDMS cross-linked network increased, the water-retention capacity of the double-layered material increased, indicating that the denser the elastomer network structure, the better it can lock and retain water.

Subsequently, a 20 day water adsorption kinetic test was conducted on the P(AM-AA)/PDMS-10 double-layered material. The results showed that within 0–10 days, as the relative humidity gradually decreased, the double-layered material lost water to the external environment, leading to a decrease in its relative mass. From 10 to 20 days, as the environmental humidity increased, the double-layered material could regenerate by absorbing water from the external environment until its weight basically returned to its initial state (Fig. 5b and c). This indicated that the double-layered material could lose or absorb

water as the environmental humidity changed, and the network structure of the double-layered material was stable and did not break down under changes in the environment. This is of great significance for the protection of unearthed ivory.

Furthermore, the water state of the P(AM-AA)/PDMS-10 double-layered material was further studied using LF-NMR technology. It was found in its  $T_2$  spectrum that the material contained two water states, namely free water and bound water (Fig. 5d).<sup>29,42</sup> Additionally, it was discovered that the proportion of bound water reached ~31% (Fig. 5e). This indicated that after silanization of the silane coupling agent, numerous strong hydrogen bonds were formed between the molecules in the double-layered material, which could reduce the vapor pressure of water in the double-layered hydrogel material; thereby imparting the hydrogel with excellent moisture retention and a slow-release performance under microenvironments. This finding is of great value for further studying the use of double-layered moisture-retaining materials for the protection of ivory.

The elephant ivory was observed before and after being unprotected, wrapped with gauze, and protected with the double-layered material using a super-depth-of-field microscope. Photographs were taken at the same location on the same piece of ivory over a period of time to observe the surface changes, which reflect the degree of dehydration and degradation. The degree of cracking and fissuring at the same location of the ivory protected with the P(AM-AA)/PDMS double-layered material changed little, and there was no significant change in its macroscopic morphology (Fig. 6a). Additionally, the adhesive strength between the hydrogel and the ivory was



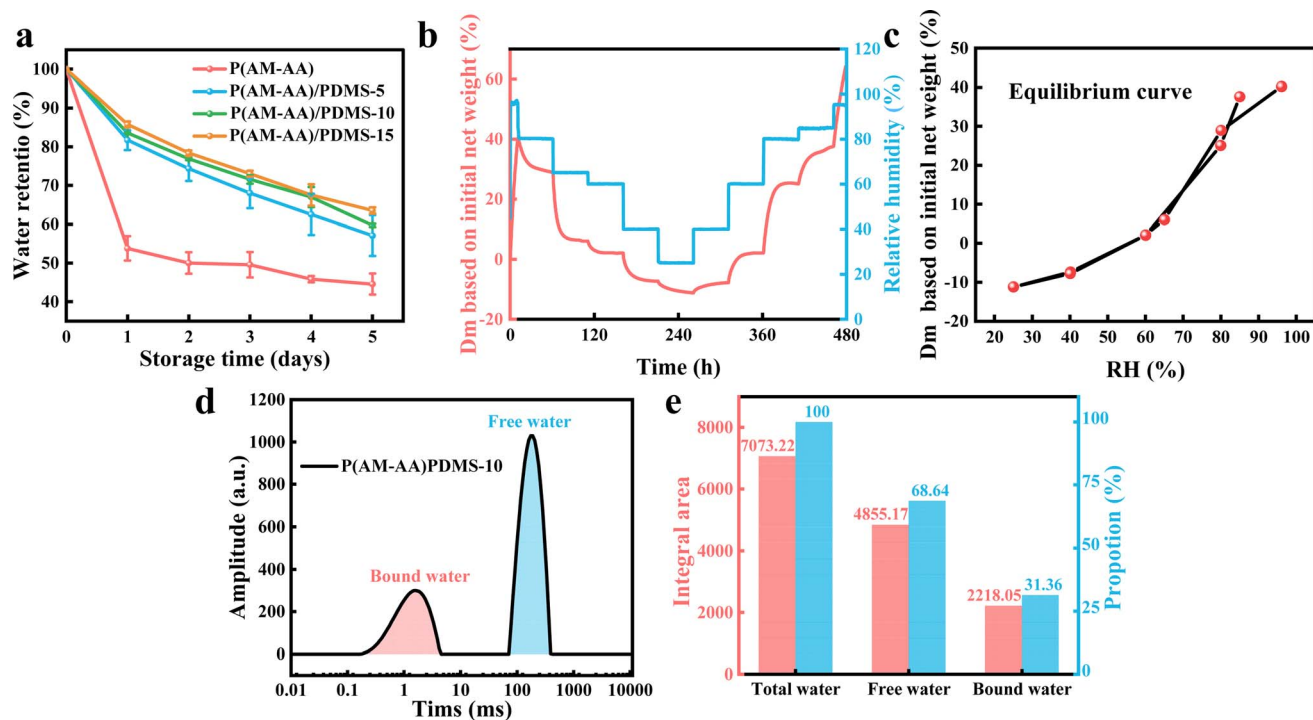


Fig. 5 (a) Weight change of the P(AM-AA) hydrogels and P(AM-AA)/PDMS double-layered material with time; (b) Kinetic adsorption curves and (c) rate of change of weight of the P(AM-AA)/PDMS-10 double-layered material during humidification and dehumidification processes; (d)  $T_2$  spectra and (e) moisture distribution of the P(AM-AA)/PDMS-10 double-layered material.

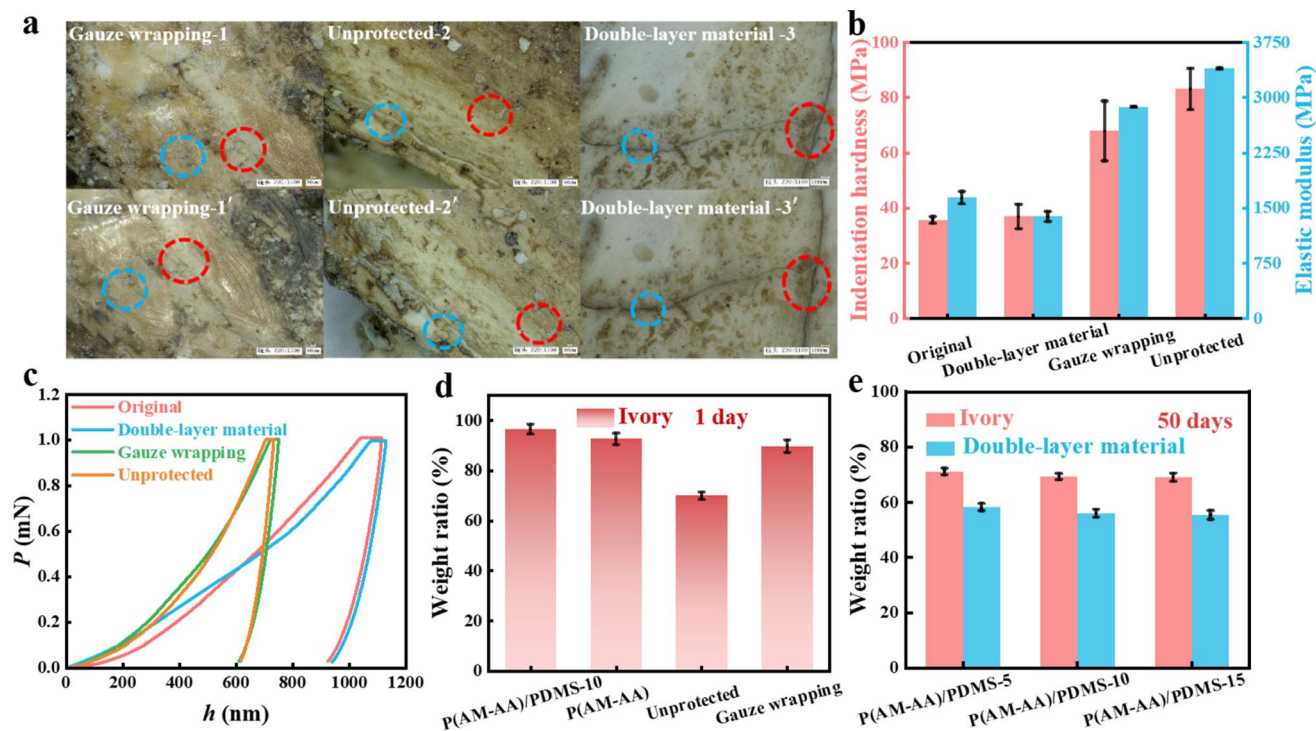


Fig. 6 (a) UltradePTH field images before and after the use of different wrappings of gauze, no protection, and the double-layered material to protect the ivory from water loss; (b) indentation hardness–elastic modulus comparison of ivory with no protection, the initial ivory, and the ivory after using the double-layered material, and gauze-wrapped technology; (c) load–displacement curves of the ivory with different treatments; (d) histogram of the weight retention rates after 1 day for the different types of ivory using different treatments; (e) histogram of the weight retention of ivory and its double-layered material coating of P(AM-AA)PDMS-5, P(AM-AA)PDMS-10, and P(AM-AA)PDMS-15 over 50 days.



relatively weak. Upon removing the double-layered protective material wrapped around the ivory, no residue of the hydrogel was found on the surface of the ivory. These findings demonstrate that the double-layered protective material could not only effectively protect the ivory but also play a significant role in moisturizing it, exhibiting a favorable effect on the *in situ* preservation of elephant ivory excavated from the Sanxingdui Ruins site.

Traditional hardness testing methods have high requirements for sample size, shape, and flatness, and can only test a sample's plastic properties. It is difficult to meet the testing conditions for the ivory samples obtained, and thus special methods need to be used. Compared with traditional hardness testing technology, nanoindentation technology can characterize the mechanical properties of materials *in situ* at the nanometer scale, and then achieve the high-precision micro-damage testing of materials.<sup>43,44</sup> In recent years, nanoindentation technology has been widely used in the quantitative characterization of the mechanical properties of materials in the interfacial regions.<sup>45</sup> We selected ivory from the K8 sacrificial pit as the research object, and calculated the indentation modulus and hardness of the ivory in the excavated pit using the Oliver–Pharr method<sup>46,47</sup> based on the principle of nano-indentation technology. Three parallel test data were obtained. The indentation hardness and elastic modulus values for the ivory protected by the double-layered hydrogel material were slightly reduced compared with the original water-saturated ivory, but the change was not significant, indicating that the double-layered hydrogel material had a certain moisturizing effect on the ivory and slowed down water loss (Fig. 6b). The mechanical properties of the ivory before and after protection were next tested to obtain the corresponding load–displacement curve. The load–displacement curve of the ivory protected by the P(AM-AA)/PDMS double-layered material changed very little (Fig. 6c). However, due to the collapse of the internal structure after water loss, the load–displacement curves of the unprotected ivory and the ivory wrapped with gauze were significantly changed. The results show that the mechanical properties of the ivory protected by the double-layered hydrogel material changed little, so it offers a good effect for the on-site preservation of ivory unearthed from the Sanxingdui site.

We chose ivory unearthed from the K8 sacrificial pit, which has the highest average water content among the four sacrificial pits, as the research object for the next part of the study. The double-layered material was directly used to wrap the ivory unearthed from the K8 sacrificial pit at the Sanxingdui site, and compared with no protection added and with wrapping with gauze as the existing technology. We studied the dehydration process of the ivory to investigate the on-site protection effect of the prepared double-layered material on the ivory unearthed from the Sanxingdui site. As shown in Fig. 6d, the water content of the ivory with no protection measure, with gauze wrapping, with the P(AM-AA) hydrogel material, and with the P(AM-AA)/PDMS double-layered material before and after one day's test was tested. It was found that the unprotected ivory lost more water, while the weight retention rate of the ivory protected by the double-layered material maintained ~95% of its weight,

which was higher than the weight retention rate (~89.5%) of the ivory with the gauze wrapping technology applied for protection. Subsequently, the weight changes of the ivory and P(AM-AA)/PDMS double-layered material were tested 50 days later (test environment temperature: 25 °C, relative humidity: 60% RH). After 50 days, the weight retention rate of the ivory remained at ~70% and the weight retention rate of the double-layered material was ~58%. Although the cross-linking density of the PDMS elastomer decreased, the water-retention rate only decreased slightly (ivory: ~69%, double-layered material: ~56%) (Fig. 6e). Notably, when the P(AM-AA) hydrogel comes into contact with ivory, the interaction between them mainly relies on the penetration and transfer of water molecules. Due to the relatively large molecular weight of the polyacrylic acid network chain, it cannot penetrate the complex structure of ivory; thus it will not cause degradation of the hydroxyapatite in ivory. After the ivory was treated with the double-layered material wrapping, there was no significant change in its surface morphology or mechanical strength. This indicates that under the used conditions, the acidic components in the hydrogel did not affect the integrity of the ivory. This finding is of great value for the on-site protection of ivory unearthed from the Sanxingdui Ruins site.

## Conclusions

In this study, a hydrophobic barrier PDMS elastomer was constructed on the surface of P(AM-AA) hydrogel using a silane coupling agent, and innovatively introduced into the temporary moisturizing protection of ivory unearthed from the Sanxingdui site. The performance of PDMS with different cross-linked network densities was investigated. By changing the concentration of components and regulating the cross-linking density and network structure of the hydrophobic barrier elastomer, a series of P(AM-AA)/PDMS double-layered materials was prepared. After manually peeling off the hydrogel, there were many gel residuals on the surface of the elastomer, and no interfacial separation occurred during the stretching process, showing its excellent interfacial bonding. In addition, the double-layer-structured composite material demonstrated a high mechanical strength of 1.2 MPa, and a water-retention rate of 60% after being placed in the air environment for 5 days, exhibiting excellent moisturizing performance. At the same time, the double-layered material also had a transmittance of more than 90%, exhibiting high transparency. The prepared P(AM-AA)/PDMS double-layered material was used to coat ivory unearthed from the Sanxingdui site. After being wrapped for 60 days, there was no significant change in the macromorphology of the ivory surface, and its mechanical properties remained basically unchanged, indicating that the coating delayed the loss of water, which plays a bonding role in the ivory. After being wrapped by the coating, the weight retention rate of the ivory after being placed for 50 days in the open environment was about 70%, indicating that the double-layered material had a significant and effective long-term on-site protection effect for the unearthed water-saturated cultural relics. This study provides ideas and a research basis



for the emergency protection and research of unearthed wet cultural relics.

## Data availability

The authors confirm that the data supporting the findings of this study are available within the article.

## Author contributions

Lang Jiang: conceptualization, validation, investigation, software, formal analysis, writing – original draft, visualization and data curation. Shilin Xiang: writing – review & editing, validation, investigation and formal analysis. Xiaoying Ji, Jinshan Lei and Dongliang Li: writing – review & editing, project administration and supervision. Sifan Li: investigation and formal analysis. Lin Xiao and Luman Jiang: conceptualization, writing – review & editing, project administration and supervision. Lijuan Zhao: resources, conceptualization, writing – review & editing, project administration and supervision. Yi Wang: resources, methodology, conceptualization, writing – review & editing, project administration, supervision, formal analysis and funding acquisition. All authors have read and agreed to the published version of the manuscript.

## Conflicts of interest

There are no conflicts to declare.

## Acknowledgements

The authors gratefully acknowledge the financial support for this work from the National Key Research and Development Program of China (Grant 2022YFF0904000), the China Tobacco Sichuan Industrial Co., Ltd (Grant cl202103), the National Natural Science Foundation of China (Grant 52203013), the Sichuan Science and Technology Program (Grant 2024NSFSC1030), and the Experimental Technology and Management Project of Sichuan Normal University of China (Grant SYJS2023010).

## References

- X. Yao and F. Zhao, *Heritage Sci.*, 2023, **11**, 93.
- Y. S. Liu, Q. M. Xu, S. F. Li, Z. B. Xie, Q. Li, H. J. Luo and S. D. Ji, *Heritage Sci.*, 2024, **12**, 90.
- Y. R. He, C. M. Huang, X. M. Xu, Y. Q. Wang and X. B. He, *J. Mt. Sci.*, 2008, **5**, 358–366.
- P. Chaynes and A. F. Mingotaud, *Surg. Radiol. Anat.*, 2004, **26**, 235–238.
- S. Zhou, X. Huang, J. Chen, X. Zheng, C. Chen and J. Chen, *Surf. Coat. Technol.*, 2024, 130503.
- M. T. Doménech-Carbó, M. Buendía-Ortuño, T. Pasies-Oviedo and L. Osete-Cortina, *Microchem. J.*, 2016, **126**, 381–405.
- Y. X. Hou, *Communications in Humanities Research*, 2023, **22**, 116–123.
- S. Correa, A. K. Grosskopf, H. Lopez Hernandez, D. Chan, A. C. Yu, L. M. Stapleton and E. A. Appel, *Chem. Rev.*, 2021, **121**, 11385–11457.
- H. L. Fan and J. P. Gong, *Macromolecules*, 2020, **53**, 2769–2782.
- X. Q. Luo, Z. Y. Yuan, X. Y. Xie, Y. J. Xie, H. Y. Lv, J. Zhao, H. Wang, Y. J. Gao, L. J. Zhao, Y. Wang and J. R. Wu, *Mater. Horiz.*, 2023, **10**, 4303–4316.
- Y. Wang, H. Y. Ouyang, Y. J. Xie, Y. N. Jiang, L. J. Zhao, W. L. Peng, J. L. Wu, J. Bao, Y. Liu and J. R. Wu, *Polymer*, 2022, **254**, 125083.
- Y. Wang, Y. J. Xie, X. Y. Xie, D. Wu, H. T. Wu, X. Q. Luo, Q. Wu, L. J. Zhao and J. R. Wu, *Adv. Funct. Mater.*, 2023, **33**, 2210224.
- B. B. Zhao, M. D. Zhao, L. M. Li, S. X. Sun, H. P. Yu, Y. Cheng, Y. D. Yang, Y. J. Fan and Y. Sun, *Int. J. Mol. Sci.*, 2022, **23**, 9962.
- T. Dutta, P. Chaturvedi, I. Llamas-Garro, J. S. Velázquez-González, R. Dubey and S. K. Mishra, *RSC Adv.*, 2024, **14**, 12984–13004.
- W. W. Li, Y. T. Wu, X. Zhang, T. K. Wu, K. K. Huang, B. Y. Wang and J. F. Liao, *RSC Adv.*, 2023, **13**, 16773–16788.
- X. Y. Xie, X. Ao, R. J. Xu, H. Y. Lv, S. Q. Tan, J. R. Wu, L. J. Zhao and Y. Wang, *Int. J. Biol. Macromol.*, 2024, 132363.
- Y. Wang, P. Y. Pan, H. Liang, J. Zhou, C. Guo, L. J. Zhao and J. R. Wu, *Biomacromolecules*, 2024, **25**, 819–828.
- T. Zhu, C. Jiang, M. L. Wang, C. Z. Zhu, N. Zhao and J. Xu, *Adv. Funct. Mater.*, 2021, **31**, 2102433.
- A. V. Torres-Figueroa, S. de los Santos-Villalobos, D. E. Rodríguez-Félix, S. F. Moreno-Salazar, C. J. Pérez-Martínez, L. H. Chan-Chan, A. Ochoa-Meza and T. del Castillo-Castro, *ACS Omega*, 2023, **8**, 44784–44795.
- H. Yuk, T. Zhang, G. A. Parada, X. Y. Liu and X. H. Zhao, *Nat. Commun.*, 2016, **7**, 12028.
- Y. K. Liu, G. M. Y. Su, R. Y. Zhang, R. J. Dai and Z. Li, *Int. J. Mol. Sci.*, 2022, **24**, 336.
- Y. Hou, N. Jiang, D. Sun, Y. P. Wang, X. C. Chen, S. S. Zhu and L. Zhang, *RSC Adv.*, 2020, **10**, 4907–4915.
- L. L. Yang, Z. T. Ou and G. C. Jiang, *Polymers*, 2023, **15**, 918.
- Y. G. Yan, J. Huang, X. Y. Qiu, X. Cui, S. L. Xu, X. W. Wu, P. Yao and C. Z. Huang, *J. Colloid Interface Sci.*, 2021, **582**, 187–200.
- D. Wirthl, R. Pichler, M. Drack, G. Kettlguber, R. Moser, R. Gerstmayr, F. Hartmann, E. Bradt, R. Kaltseis, C. M. Siket, S. E. Schausberger, S. Hild, S. Bauer and M. Kaltenbrunner, *Sci. Adv.*, 2017, **3**, e1700053.
- Z.-q. Zhang, K.-f. Ren and J. Ji, *Biointerphases*, 2023, **18**, 030801.
- L. Wang, G. Y. Xie, X. Mi, B. Zhang, Y. Du, Q. Y. Zhu and Z. C. Yu, *ACS Omega*, 2023, **8**, 20116–20124.
- T. Aziz, A. Ullah, H. Fan, M. I. Jamil, F. U. Khan, R. Ullah, M. Iqbal, A. Ali and B. Ullah, *J. Polym. Environ.*, 2021, **29**, 3427–3443.
- F. Ilmain, T. Tanaka and E. Kokufuta, *Nature*, 1991, **349**, 400–401.



- 30 L. Nie, Q. Wei, J. Li, Y. Deng, X. He, X. Gao, X. Ma, S. Liu, Y. Sun, G. Jiang, O. V. Okoro, A. Shavandi and S. Jing, *RSC Adv.*, 2023, **13**, 8502–8522.
- 31 M. Litwinowicz, S. Rogers, A. Caruana, C. Kinane, J. Tellam and R. Thompson, *Macromolecules*, 2021, **54**, 9636–9648.
- 32 R. Moučka, M. Sedláčik, J. Osíčka and V. Pata, *Sci. Rep.*, 2021, **11**, 19090.
- 33 H. B. Zhang, X. Huang, J. X. Jiang, S. B. Shang and Z. Q. Song, *RSC Adv.*, 2017, **7**, 42541–42548.
- 34 Q. H. Liu, G. D. Nian, C. H. Yang, S. X. Qu and Z. G. Suo, *Nat. Commun.*, 2018, **9**, 846.
- 35 J. Huang, X. Y. Qiu, B. Yan, L. Xie, J. Q. Yang, H. L. Xu, Y. H. Deng, L. Y. Chen, X. G. Wang and H. B. Zeng, *J. Mater. Chem. B*, 2018, **6**, 3742–3750.
- 36 D. R. Biswal and R. P. Singh, *Carbohydr. Polym.*, 2004, **57**, 379–387.
- 37 F. Yang, X. Wang, Q. L. Hu, D. D. Jiang, Y. Lu, Y. Wang, J. H. Wang and J. H. Liu, *Mater. Chem. Front.*, 2021, **5**, 6491–6501.
- 38 X. X. Zhang, B. B. Xia, H. P. Ye, Y. L. Zhang, B. Xiao, L. H. Yan, H. B. Lv and B. Jiang, *J. Mater. Chem.*, 2012, **22**, 13132.
- 39 L. M. Johnson, L. Gao, C. W. Shields Iv, M. Smith, K. Efimenko, K. Cushing, J. Genzer and G. P. López, *J. Nanobiotechnol.*, 2013, **11**, 1–8.
- 40 J. J. H. Lancastre, N. Fernandes, F. M. A. Margaça, I. M. Miranda Salvado, L. M. Ferreira, A. N. Falcão and M. H. Casimiro, *Radiat. Phys. Chem.*, 2012, **81**, 1336–1340.
- 41 B. Li, H. B. Qin, M. Ma, X. J. Xu, M. J. Zhou, W. R. Hao and Z. G. Hu, *RSC Adv.*, 2023, **13**, 5667–5673.
- 42 L. Liu, Z. He, X. H. Cai and S. J. Fu, *Appl. Magn. Reson.*, 2020, **52**, 15–31.
- 43 G. Mallikarjunachari, T. Nallamilli, P. Ravindran and M. G. Basavaraj, *Colloids Surf., A*, 2018, **550**, 167–175.
- 44 P. C. Zhu, Y. J. Zhao, S. Agarwal, J. Henry and S. J. Zinkle, *Mater. Des.*, 2022, **213**, 110317.
- 45 Y. Gaillard and F. Amiot, *Composites, Part A*, 2020, **132**, 105807.
- 46 W. C. Oliver and G. M. Pharr, *J. Mater. Res.*, 1992, **7**, 1564–1583.
- 47 W. C. Oliver and G. M. Pharr, *J. Mater. Res.*, 2004, **19**, 3–20.

